This article was published as: journal of the mechanical behavior of biomedical materials 104 (2020) 103619. DOI: https://doi.org/10.1016/j.jmbbm.2020.103619

In vitro characterization of a novel magnetic fibrin-agarose hydrogel for cartilage tissue engineering

Autores:

Ana Belén Bonhome-Espinosa,[1 2] Fernando Campos, [2 3] Daniel Durand-Herrera, [2 3] José Darío Sánchez-López,[4] Sébastien Schaub,[5] Juan D. G. Durán,[1 2] Modesto T. Lopez-Lopez,[* 1 2] Víctor Carriel [2 3]

Affiliation:

[1]Department of Applied Physics, University of Granada, Faculty of Science, Campus de Fuentenueva, 18071 Granada, Spain.
[2]Instituto de Investigación Biosanitaria Ibs.GRANADA, Granada, Spain.
[3]Department of Histology & Tissue Engineering Group, Faculty of Medicine, University of Granada, Spain.
[4]Division of Maxillofacial Surgery. University Hospital Complex of Granada. Granada, Spain.
[5]Université Côte d'Azur, CNRS, INSERM, Inria, iBV, France.

*Corresponding author: modesto@ugr.es

Abstract:

The encapsulation of cells into biopolymer matrices enables the preparation of engineered substitute tissues. Here we report the generation of novel 3D magnetic biomaterials by encapsulation of magnetic nanoparticles and human hyaline chondrocytes within fibrin-agarose hydrogels, with potential use as articular hyaline cartilage-like tissues. By rheological measurements we observed that, (i) the incorporation of magnetic nanoparticles resulted in increased values of the storage and loss moduli for the different times of cell culture; and (ii) the incorporation of human hyaline chondrocytes into nonmagnetic and magnetic fibrin-agarose biomaterials produced a control of their swelling capacity in comparison with acellular nonmagnetic and magnetic fibrin-agarose biomaterials. Interestingly, the *in vitro* viability and proliferation results showed that the inclusion of magnetic nanoparticles did not affect the cytocompatibility of the biomaterials. What is more, immunohistochemistry showed that the inclusion of magnetic nanoparticles did not negatively affect the expression of type II collagen of the human hyaline chondrocytes. Summarizing, our results suggest that the generation of engineered hyaline cartilage-like tissues by using magnetic fibrin-agarose hydrogels is feasible. The resulting artificial tissues combine a stronger and stable mechanical response, with promising *in vitro* cytocompatibility. Further research would be required to elucidate if for longer culture times additional features typical of the extracellular matrix of cartilage could be expressed by human hyaline chondrocytes within magnetic fibrin-agarose hydrogels.

Key words:

Hyaline cartilage, fibrin-agarose, magnetic nanoparticles, cell-biomaterial interactions, biomechanical properties, tissue engineering.

1. Introduction

Hyaline cartilage is a non-vascularized connective tissue consisting of chondrocytes immersed in an abundant and highly specialized extracellular matrix (ECM) mainly composed of type II collagen and proteoglycans.[1-4] In adult musculoskeletal systems, hyaline cartilage constitutes two specialized structures, the articular cartilage and the growth plate.[2, 5] The articular cartilage is essential for the musculoskeletal biomechanics, allowing sliding and rotation of diarthrosis during exercise. In the case of the growth plate, it is a transitory cartilaginous structure responsible for the growth and elongation of bones during childhood.[4]

Cartilage can be affected by several pathological conditions such as infectious diseases, osteoarthritis, cancer and traumatic injuries [6]. Furthermore, inadequate or excessive mechanical loads can progressively damage the articular cartilage structure and function with severe and mostly irreversible consequences on these patients.[1, 3, 7-9] In this context, it was demonstrated that more than 60 % of young patients undergoing arthroscopic procedures have lesions in the articular hyaline cartilage. [10, 11] Unfortunately, cartilage has limited spontaneous regeneration capability, mainly due to the absence of vascularization and its complex ECM 3D organization. Currently, different techniques are available for cartilage repair, such as microfracture, ACI (autologous chondrocyte implantation) and MACI (matrix-assisted autologous chondrocyte implantation).[12] These strategies have been shown promising, especially through the combination of hydrogels and cells,[13] and therefore more research must be done to improve the structure and function of articular cartilage.

Considering the promising results obtained by tissue engineering in this field, we hypothesized that the generation of novel magnetic hydrogels that ensure cell function and provide adequate biomechanical properties and hydration to the regenerative microenvironment could be useful for the artificial regeneration of native cartilage. For the exploration of this hypothesis, we chose fibrin-agarose hydrogels (FAH) due to their positive results in the generation of many other engineered bio-artificial substitutes, such as skin, oral mucosa, peripheral nerves, cornea and scleral substitutes.[14] In addition, these hydrogels have been successfully used for the encapsulation of elastic cartilage-derived chondrocytes, ensuring the viability and functionality of these cells *in vitro*.[15] Our decision to embed magnetic nanoparticles (MNP) within the chosen FAH was based in previous studies that support the hypothesis of improving the mechanical properties of biomaterials containing MNP.[16] Additionally, other advantages have been reported for magnetic hydrogels in the field of tissue engineering, such as the improvement of cell culture efficiency of some types of cells such as fibroblasts [17, 18] and the stimulation of adhesion, proliferation, and differentiation of cells *in vitro*, and even bone formation *in vivo* [19-22].

In view of the previous discussion, the goal of this paper is twofold. First, the study of the biomechanical changes (storage (G') and loss (G'') moduli) due to the MNP or/and chondrocytes embedded in the biomaterials. Second, the study of *in vitro* viability of chondrocytes within both magnetic and nonmagnetic fibrin-agarose hydrogels; as well as preliminary histochemical and immuhistochemical analyses to determinate the influence of MNP in the cell-biomaterial interaction

and to identify expression of ECM native hyaline cartilage proteins by the chondrocytes embedded in these new magnetic biomaterials.

2. Materials and methods

We generated novel 3D magnetic cartilage-like fibrin-agarose constructs (3D-MCFAC) for cartilage tissue engineering. These bio-artificial substitutes were subjected to biomechanical characterization (by using rheological techniques), followed by a complete biochemical and histological evaluation of the cell viability and functionality during 30 days of *ex vivo* development (EVD).

2.1. Human hyaline-derived chondrocytes isolation and expansion

Human hyaline-derived chondrocytes (HHC) were isolated from small biopsies from two healthy donors subjected to nasal surgeries (under informed consent). Biopsies were mechanically fragmented and then subjected to enzymatic digestion with 2 mg/mL of *Clostridium histolyticum* type II collagenase (Gibco BRL Life Sciences Technologies) at 37 °C, following previously described methods [15, 23]. Cells were expanded until passage 6 with DMEM/F-12 culture medium supplemented with 10 % of fetal bovine serum, 1 % of antibiotic and antimycotics cocktail solution, 2 mM L-glutamine (all from Sigma-Aldrich) as previously described [15, 23].

2.2. Generation of 3D-MCFAC and experimental groups

We generated different bio-artificial substitutes based on the use of FAH which could contain HHC and/or MNP (we used MagP-OH® magnetic nanoparticles supplied by NanoMyp®, Spain). As indicated by the manufacturer, these magnetic nanoparticles consisted of 90 % v/v of a multicrystalline magnetite (iron oxide) core and a 10 % v/v of polymeric layer (composed by 54 wt % methyl methacrylate, 15 wt % hydroxyl ethyl methacrylate and 31 wt % ethylene glycol dimethacrylate) functionalized with OH groups. This surface functionalization confers negative charge to the particle surface in water, due to the OH^- groups. These particles are roughly spherical and possess a hydrodynamic diameter of 110 nm, as measured by dynamic light scattering with a Zetasizer instrument (Malvern instruments, USA) –see Ref. [24]. To prepare 20 mL of fibrin-agarose biomaterial we mixed 15.2 mL of human plasma (supplied by the Public Health System Biobank of Granada, Spain) with 2.5 mL of chondrogenic culture medium (containing 5×10^4 HHC/mL in the case of cellular biomaterials), and 300 µL of tranexamic acid (Fides-Ecofarma, Valencia, Spain) that prevented from fibrinolysis. We mixed this mixture carefully, and afterwards we added 2 mL of a 1 % w/v $CaCl_2$ solution (to promote the gelation) and 1 mL of a 2 % w/v type VII-agarose (Sigma Aldrich) solution. We mixed carefully the resulting mixture and then kept aliquots of it at 37°C in 60 mm Petri dishes until complete gelation. In the case of biomaterials containing MNP, we incorporated them within the culture medium at the required concentration, so that the final concentration of MNP in the total volume of biomaterial was 0.1 % v/v. To conclude, the experimental groups and controls were as it follows:

(i) a-FAH control: Biomaterials without cells and without MNP.

(ii) c-FAH control: Biomaterials without MNP, containing cells at a concentration of 5 x 10^4 HHC/mL.

(iii) a-MFAH: Biomaterials without cells, containing MNP at a concentration of 0.1 % v/v.

(iv) c-MFAH: Biomaterials containing MNP at a concentration of 0.1 % v/v and cells at a concentration of 5 x 10^4 HHC/mL.

All biomaterials were kept under standard culture conditions (37 °C and 5 % CO_2) in chondrogenic medium during 30 days. We changed the chondrogenic medium every three days. The chondrogenic medium used in this study was composed by DMEM/F-12, with 0.1 % of antibiotics cocktail solution, 2 mM of sodium pyruvate (GIBCO), 0.1 % volume ITS (insulin-transferrin-sodium selenite), 4 µM ascorbic acid, 10 ng·mL^{-1} of human TGF-β1 (transforming growth factor-β1 human), 10 µM of dexamethasone and 0.35 mM L-proline (all from Sigma-Aldrich, Germany).[25]

Fig. 1. Macroscopic appearance of FAH without (left) and containing (right) MNP. Hydrogels without MNP presented a pink colour due to the culture medium, while hydrogels containing MNP acquired a characteristic brown colour.

2.3. Biomechanical characterization

We characterized the biomechanical properties of the four experimental groups of biomaterials based on the use of fibrin-agarose hydrogels (a-FAH control, c-FAH control, a-MFAH and c-MFAH) with a Haake MARS III controlled-stress rheometer (Thermo Fisher Scientific, Walthman, MA, USA) at 37 °C. The measuring system geometry was a set of parallel disks made of titanium with 3.5 cm of diameter and rough surface to avoid wall slip on the measuring surfaces (sensor P35Ti L, Thermo Fisher Scientific, Waltham, MA, USA). In order to ensure that the upper disk was in perfect contact with the sample, it was lowered slowly until the normal force exerted on the measuring disk reached a value between 0.25 and 1.0 N, thus ensuring that the compression exerted on the sample was weak. The volume of pre-gel mixture used for the preparation of each sample was 3 mL. Note that the prepared biomaterials had the same disk-like shape that the measuring geometry due to the fact that the biomaterials were prepared in culture dishes of 3.5 cm of diameter –Fig. 1. To avoid water evaporation during rheological measurements, we created a supersaturated water atmosphere around the measuring geometry, by using a small home-made cap situated around the sample and with a single hole for the introduction of the axis of the upper plate of the rheometer. The lower plate of the rheometer was connected to a water thermostatic bath that allowed

controlling the temperature of the measuring system. Due to the little combined volume of the sample (0.4 – 1.6 mL), the upper plate of the rheometer and the atmosphere enclosed by the cap, the temperature of 37 °C was approximately reached and maintained within the whole measuring system after 3 minutes of placing the sample in it. We waited always this time before rheological measurements were conducted.

We studied the dynamic response of the biomaterials by subjecting them to a sinusoidal shear strain, $\gamma(t)$, of given amplitude, γ_0, and frequency, *f*, and by measuring the corresponding shear stress, $\sigma(t)$. We performed two types of tests for this regime: (i) Amplitude sweeps, for which we set the frequency of the sinusoidal shear strain to a value *f*=1 Hz and increased its amplitude logarithmically in the range $\gamma_0 = 1 \times 10^{-4} - \gamma_0 = 2.0$. This test allowed us to delimit the linear viscoelastic region (LVR). (ii) Frequency sweeps, for which we set the amplitude of the sinusoidal shear strain to a value within the LVR, and increased the frequency linearly in the range 0 – 1 Hz.

2.4. Cell viability assessment

We analyzed the viability and functionality of the chondrocytes cultured in FAH-based biomaterials (c-FAH and c-MFAH) by WST-1 assay. Furthermore, we quantified the released DNA by previously described methodology.[24, 26] We carried out these analyses at 2, 9, 16 and 30 days of EVD. We also carried out the same analyses for the acellular biomaterials (a-FAH and a-MFAH) and used the results as technical controls (data not shown).

The WST-1 (Cell Proliferation Reagent WST-1, Roche Diagnostics, Germany) assay consists of the transformation of tetrazolium salt (WST-1) to formazan (colorimetric reaction) by the activity of the mitochondrial dehydrogenase. This activity is directly proportional to the number of viable and metabolically active cells. For this assay cells were cultured with the working solution for 4 h at 37 ^{o}C, and then we determined the absorbance of the colorimetric reaction with an Assay UVM 340 spectrophotometer in triplicate.

We quantified the DNA released by the cells in the culture medium during culture with a NanoDrop 2000 UV–Vis Spectrophotometer (Thermo Fisher Scientific) as previously described.[26, 27] The release of DNA from cells in culture occurs as a consequence of irreversible damage of the cell membrane and, therefore, higher values of DNA in the culture medium indicate a high degree of cell mortality. In this sense, 10 µL of the culture medium was harvested and used to determine the amount of DNA for each condition and time. For this analysis we used five independent samples from each condition, and quantified each sample three times (n=15 for each condition).

Finally, for WST-1 and DNA quantitative analyses, we used as positive technical control (Positive CTR group) cells cultured under 2D conditions. For this purpose, we seeded 5 x 10^4 HHC in 1 mL of culture medium within a culture dish and afterwards HHC were cultured under the same conditions that hydrogel-based samples. Note that the concentration of cells in 2D cultures was the same as in hydrogels. Furthermore, as negative technical controls (Negative CTR group) we used c-FAH, c-MFAH and 2D cell cultures incubated with 1 % Triton X-100, to induce an irreversible cell-membrane damage and DNA release.

2.5. Histological cell-biomaterial interaction analyses

We conducted histological studies in cellular hydrogels (c-FAH and c-MFAH) at 2, 9, 16 and 30 days of EVD. For these analyses we harvested the samples and fixed them in 4 % neutral buffered formaldehyde for 48 h at room temperature. Fixed samples were dehydrated, cleared and embedded in paraffin by using a protocol for delicate tissue samples.[28] Embedded tissues were sectioned at 5 µm and used for histological, histochemical and immunohistochemical analyses.

Histological analyses were performed by using hematoxylin-eosin technique, which in the case of c-MFAH was also combined with Perl's histochemical method following a previously described procedure.[17] The identification of acid proteoglycans was carried out with Alcian blue histochemical method at pH 2.5 (contrasted with nuclear fast red).[15] Furthermore, S-100 protein (chondrocyte marker) and type II collagen (cartilage-specific extracellular matrix molecule) were identified by using indirect immunohistochemistry (IHC) as described previously.[15] For IHC the primary antibody was omitted in one section and used as negative technical control. S-100 protein was identified with a rabbit anti-S100 polyclonal antibody (Dako Cytomation, Glostrup, Denmark. Product number: Z0311) whereas the type II collagen was identified with a rabbit anti-collagen II polyclonal antibody (EMD Millipore, Billerica, Massachusetts, USA; Product number: AB2036).[19]

In this study, we determined the cellularity in c-FAH and c-MFAH over time following a previously described procedure.[29] Briefly, we determined the number of cells in a specific area (1.24 mm^2) in each condition. We made three determinations in each section and evaluated three sections of one independent sample per group and time.

We analyzed the cell-biomaterial interactions of the histological sections using a microscope ZEISS Axioplan2 (Carl Zeiss Microscopy GmbH, Jena, Germany) equipped with lens 25x/0.8 Oil and 63x/1.4 Oil. Images were acquired with an Infinity 3-6 Lumenera color camera (Lumenera Corporation, Ottawa, Canada) controlled by MicroManager 1.4.[30]

2.5.1. Statistical analyses

We subjected quantitative values from cell viability and cellularity analyses to Shapiro Wilk test of normality by using SPSS 16.0 software. In this sense, we used Mann-Whitney non-parametric test to determine statistically significant differences among experimental conditions and controls. In this paper we show quantitative values as mean ± standard deviation, and $p<0.05$ is considered statistically significant.

2.6. Ethics statement

This study was approved by the Ethics Committee of the University of Granada, Granada, Spain. Each tissue donor signed an informed consent form for the study.

3. Results and discussion

3.1. Biomechanical characterization

The rheological behavior of the fibrin-agarose biomaterials (a-FAH, c-FAH, a-MFAH and c-MFAH) was characterized by subjecting them to oscillatory shear strain. With this aim, the shear stress experienced by the biomaterials under a sinusoidal shear strain, with a certain frequency and amplitude, was recorded.

First, we obtained the corresponding amplitude sweeps of the four experimental groups. For this aim, we carried out oscillatory shear tests of fixed frequency (1 Hz) and increasing shear strain amplitude and monitored the resulting shear stress. From these data we obtained the values of the storage (*G'*) and loss (*G"*) moduli as functions of the strain amplitude (γ_0). Fig. 2 illustrates the typical trends for the curves of *G*' and *G*'' vs. γ_0, as well as for the curves of *G*' and *G*'' vs. the amplitude of the shear stress (σ_0) –similar trends were obtained for all the four experimental groups. The obtained curves show approximately constants values of *G'* and *G"* at low shear strain amplitude (γ_0 < 0.01). This region is known as linear viscoelastic region (LVR). In this region the values of *G'* were higher than the values of *G"*, a typical behavior of a viscoelastic solid. At larger values of shear strain amplitude, *G*' presented a strong decrease, whereas *G*'' first increased to a maximum (yield point) and then decreased strongly too. This region is known as nonlinear viscoelastic region. Within this region of decreasing *G*' and *G*'', we observe that the *G'* and *G"* curves began to converge (until there was a crossover between both curves at γ_0 = 0.9. Above this value of the shear strain amplitude, *G"* > *G'*, indicating that the dissipated energy (≈ *G"*) was higher than the storage elastic energy (≈ *G'*). This fact was due to the breakage of the internal structure of the hydrogel at the microscopic scale. Similar conclusions can be drawn from the analysis of the curves of *G*' and *G*'' vs. σ_0.

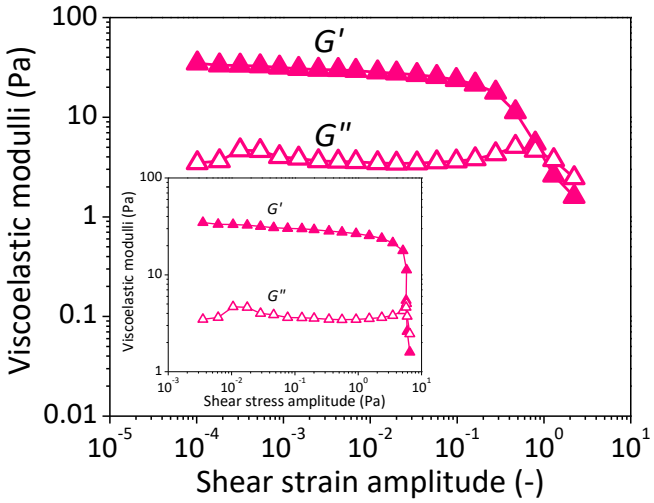

Fig. 2. Storage (*G*') and loss (*G*") moduli as functions of the shear strain amplitude (at a constant frequency of 1 Hz) for cellular fibrin-agarose biomaterial (c-FAH) at 16 days of cell culture. Inset shows storage (*G*') and loss (*G*") moduli as functions of the shear stress amplitude.

In order to compare the time evolution of the viscoelastic moduli in the four experimental groups (a-FAH, c-FAH, a-MFAH and c-MFAH), we obtained the average values of *G'* and *G"* corresponding to the LVR (10^{-4} < γ_0 < 0.01) as functions of the time (Fig. 3). As observed, for nonmagnetic and magnetic acellular fibrin-agarose biomaterials (Fig. 3a) *G'* and *G"* decreased with time, showing the most pronounced decrease (especially for *G'*) between day 2 and day 16. In contrast, *G'* and *G"*

remained practically stable, with even a progressive and slight increase in *G'* for the time interval under study (days 2 to 30) for the nonmagnetic and magnetic cellular fibrin-agarose biomaterials (Fig. 3b).

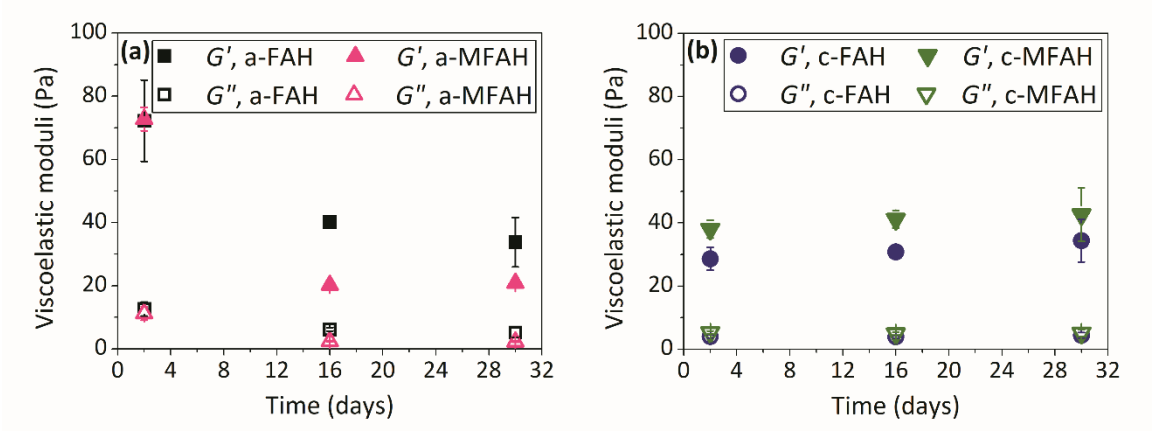

Fig. 3. Storage (*G'*) and loss (*G''*) moduli, corresponding to the linear viscoelastic region, as a function of culture time: (a) Nonmagnetic (a-FAH) and magnetic (a-MFAH) acellular fibrin-agarose biomaterials; (b) Nonmagnetic (c-FAH) and magnetic (c-MFAH) cellular fibrin-agarose biomaterials.

In order to give an explanation to the contradictory behavior between acellular and cellular groups observed in Fig. 3, it is necessary to analyze the data in this figure in view of the volumes of biomaterial contained between the upper and the bottom disks of the rheometer. For this aim, we monitored the distances between the measuring disks of the rheometer, and from these data we obtained the volume of the cylindrical samples contained between the rheometer disks (Fig. 4). As observed, for acellular biomaterials (Fig. 4a) the nonmagnetic ones (a-FAH) had a volume about three times smaller than the magnetic ones (a-MFAH), a difference that was maintained from day 1 to day 30. This result agrees with our previous work for fibrin hydrogels,[24] where we reported increase swelling for magnetic hydrogels with respect to nonmagnetic ones. The higher volume of fibrin-based magnetic biomaterials with respect to nonmagnetic ones was explained by a more opened microstructure of the former due to the formation of network knots by the MNP, which resulted in a greater capacity for swelling by absorption of aqueous solution –for more details see Ref. [24]. In contrast, for cellular biomaterials (Fig. 4b), we observed that MNP had a negligible impact in the volume of the resulting biomaterials (compare data for c-FAH and c-MFAH) and, interestingly, that for cellular biomaterials there was a decrease in volume as the culture time increased. Both differences with respect to the behavior of acellular biomaterials should be connected to the role of HHC, and in consequence we may conclude that there was a cell-mediated contraction of the biomaterials that was already noticeable at day 2, and more evident at day 30.

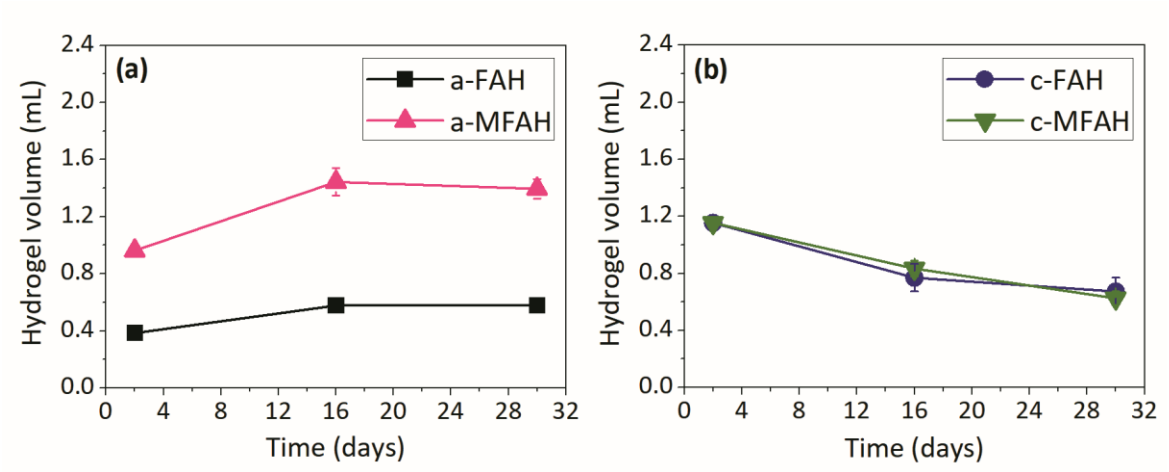

Fig.4. Biomaterial volume as a function of culture time, for samples used for the rheological characterization, as estimated from the distance between the upper and lower plates of the rheometer. (a) Acellular biomaterials; (b) cellular biomaterials.

A correct interpretation of the data of Fig. 3 can now be done in the framework of results of Fig. 4. For this aim and in view of the differences in volume between experimental groups and culture times, it seems reasonable to normalize the values of the viscoelastic moduli by the volume fraction of polymer in the biomaterials. This normalization is supported by the classical theory of elasticity of gel networks, which demonstrates a direct relation between elasticity of the gels and the concentration of polymer threads –see for example Ref. [31]. Then, since the amount of polymer (fibrin plus agarose) is the same in all experimental groups, this normalization, which is equivalent to the multiplication of the viscoelastic moduli by the volume of the hydrogels (Fig. 5), allows getting more correct information about the role of cells.

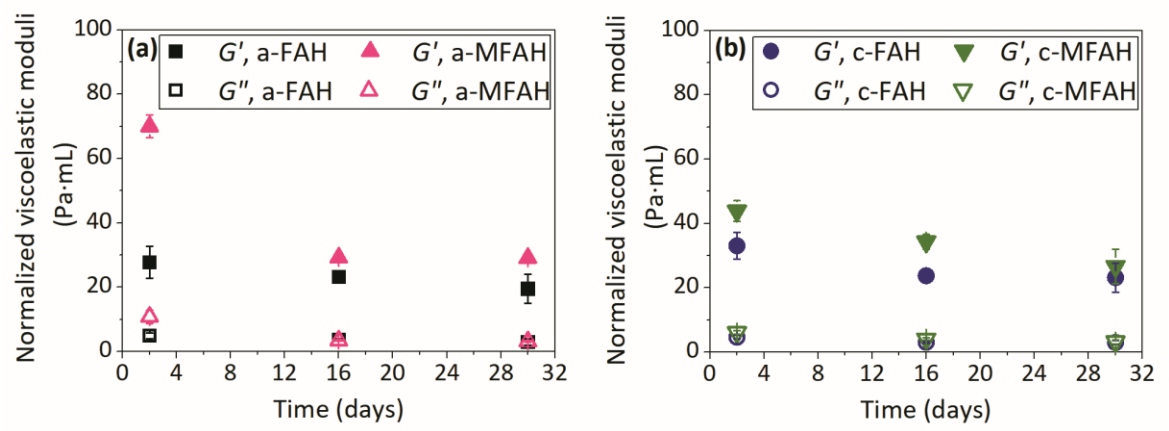

Fig. 5. Normalized storage (a) and loss (b) moduli as functions of time for all the experimental groups of fibrin-agarose biomaterials (indicated in the graphs). Values of storage and loss moduli presented in the graph are the mean values within the LVR. Normalized values were calculated from the product of each value of viscoelastic moduli times the corresponding hydrogel volume.

Normalized results of the viscoelastic moduli are shown in Fig. 5. As observed, the normalized values decreased for all experimental groups, something that might be connected with some degradation

of the polymers. Nevertheless, since in cellular biomaterials a proportional reduction of volume took place, we could conclude that cells stabilized the hydrogels. Concerning the precise role of cells in the normalized viscoelastic moduli, as can be inferred from Fig. 5 (compare parts a and b), it seems to be almost negligible with the exception of magnetic samples at day 2, for which a much larger value was obtained for the acellular hydrogel –we do not have a clear explanation for this discrepancy. Note finally that in spite of normalization by hydrogel volume, magnetic samples still demonstrated higher normalized viscoelastic moduli than nonmagnetic samples, corroborating the positive role of MNP for the improvement of the mechanical properties.

We also performed oscillatory tests of fixed shear strain amplitude within the LVR (γ_0= 0.001) and increasing frequency in the range 0 to 1 Hz. From these measurements we obtained the viscoelastic moduli as a function of the frequency. Normalized values of the viscoelastic moduli are plotted vs. frequency in Fig. 6 –note that this normalization does not change the shape of the curves, but only their relative value. As observed, all samples demonstrated a solid-like viscoelastic behavior, characterized by *G*' and *G*'' values approximately independent of frequency, with *G*' values considerably larger than *G*''. Indeed, this behavior is typical of cross-linked polymer systems.[32]

In addition, from data of Fig. 6, we could conclude that the weakest normalized elastic response (lowest normalized *G*' values) was this of the cellular nonmagnetic sample, whereas the strongest response was shown by the cellular magnetic sample, supporting the strengthening induced by the presence of MNP –note that differences between normalized data for samples c-MFAH and c-FAH are statistically significant.

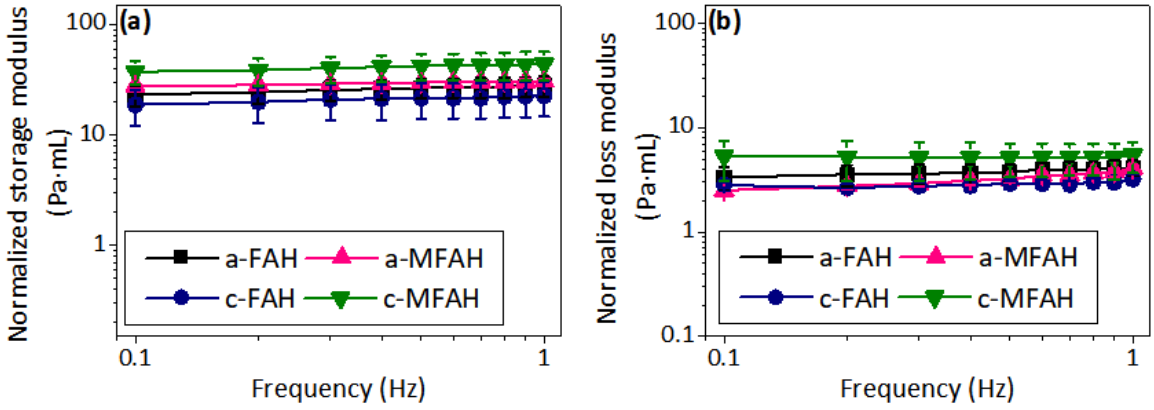

Fig. 6. Normalized storage (a) and loss (b) moduli as functions of frequency for all the experimental groups of fibrin-agarose biomaterials (indicated in the graphs) at 16 days of culture –similar trends were obtained for 2 and 30 days of cell culture. Normalized values were calculated from the product of each value of viscoelastic moduli times the corresponding hydrogel volume.

Let us finally comment on the magnitude of the elastic response of the biomaterials. As observed in Fig. 3, values of the storage modulus, *G*', within the LVR were mostly in the range 20-40 Pa for the different samples and, due to their predominantly elastic response (*G*' > *G*''), the magnitude of the complex rigidity modulus, $|G^*| = [(G')^2 + (G'')^2]^{0.5}$, was also within the same range; note that in

oscillatory shear $\sigma(t) = G^*\gamma(t)$. [33] These low values of $|G^*|$ would allow easily implantation of these biomaterials, for example by injection, but on the other hand, these values are much lower than the values reported in literature for the rigidity modulus (*G*) of the natural human articular hyaline cartilage; note that *G* is the ratio of shear stress to the shear strain, $G = \frac{\sigma}{\gamma}$, obtained from steady state measurements within the linear elastic regime. Therefore, ***G**** equals *G* in the limit of frequency tending to zero. Stammen *et al*. collected a *G* value of 0.23 MPa.[34] Other authors such as Magnussen *et al*. gave values of *G* between 1 and 3 MPa depending on shear conditions, although with a large standard deviation (for example, for a strain rate of 0.01 s^{-1}, *G* = 1.05 ± 0.84 MPa).[35]

3.2. Cell viability assessment

Abundant HHC were successfully isolated with the use of collagenase digestion. Some characteristics of these cells were their abundant cytoplasm and the formation of elongated lamellipodium and filopodium. As the time of cell culture increased (trypsinization and passage) HHC acquired a characteristic polygonal shape with an abundant cytoplasm (Fig. 7).

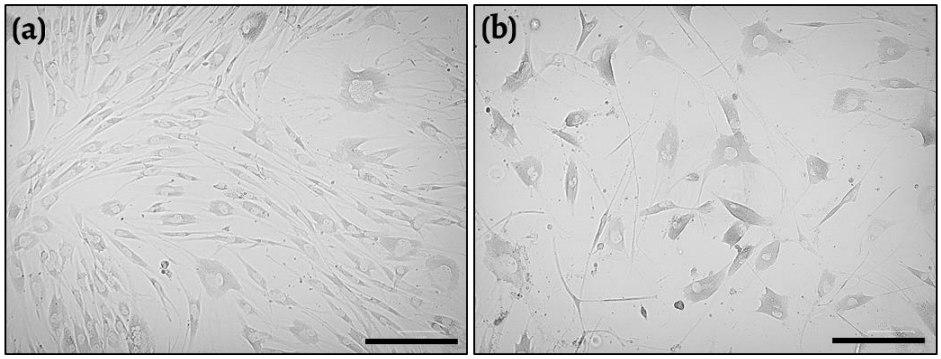

Fig. 7. Phase contrast microscopy of primary HHC cell culture (a) and after the first passage (b). Note the characteristic polygonal shape and abundant cytoplasm of these cells, especially when they were subcultured. Scale bar= 200 µm.

The WST-1 assay was used to quantitatively determine the cellular metabolic activity of HHC cultured in each biomaterial (c-FAH and c-MFAH) and in standard 2D culture conditions (positive and negative controls) –see Fig. 8. WST-1 at 2 days of EVD revealed significantly higher absorbance values in 2D positive control than in other experimental conditions ($p<0.05$). Cell metabolic activity values resulted comparable between c-FAH and c-MFAH groups, and for both conditions it was significantly higher than for the negative control ($p<0.05$). With the advance of the EVD time, a clear and significant decrease of WST-1 values was observed in the positive control group ($p<0.05$), with values significantly lower than for c-FAH and c-MFAH groups for days 9, 16 and 30. Interestingly, a significant and progressive increase of the cellular metabolic activity was observed in c-FAH and c-MFAH groups during the 30 days of the study ($p<0.05$). These values were significantly higher in c-FAH than in c-MFAH at day 9 ($p= 0.05$) and at day 16 ($p= 0.05$). WST-1 at 30 days showed slightly higher values in c-FAH than c-MFAH group, but this difference was not statistically significant ($p= 0.05$) –see Fig. 8.

These results demonstrate that HHC needed some days to adapt their metabolism and function to a new 3D microenvironment, in this case to the FAH alone or containing MNPs. Time-course analysis clearly reveals that HHC were adapted faster to FAH than to MFAH, but differences were not significant after 30 days, demonstrating that FAH and MFAH successfully supported an active metabolic activity of HHC under chondrogenic culture conditions. It should be noted that for both groups (FAH and MFAH), in parallel with the increase of the cellular metabolic activity with time, there was a significant reduction of the volume of the biomaterials (Fig. 4b), likely as a consequence of cell-mediated contraction. Furthermore, as an additional consequence of cell proliferation, and the resulting cell-mediated contraction, the net strength (before normalization – see Fig. 3b) of the cellular samples increased, in spite of the degradation of the polymers that seemed to take place over time (see Fig. 5). The significant decrease of WST-1 values in positive control is explained by the fast proliferation and contact inhibition of these cells under 2D culture conditions, highlighting the importance of a 3D microenvironment for the function of these cells.

The quantitative normalized results of the DNA released by the HHC, as an indicator of irreversible cell damage, showed significantly lower values in both experimental groups and the positive control than in the negative control group (100 %) –Fig. 9. When c-FAH and c-MFAH were analyzed, a scarce and not significant increase of DNA values was observed at 9 days of EVD, but these values did not even reach 2 % of the DNA content. Furthermore, 0 % of DNA was released from HHC cultured in c-FAH or c-MFAH at 16 and 30 days demonstrating the high cytocompatibility of the biomaterial and MNPs used. These results clearly demonstrated that the MNP did not affect cell viability and functionality over the time, something that is also supported by the progressive and significant increase of cell metabolic activity observed with WST-1 assay during the 30 days analyzed. This conclusion is also in agreement with the high cytocompatibility of the FAH for encapsulation of human elastic cartilage-derived chondrocytes, observed in our previous works. [15] And it is also supported by previous cytocompatibility studies of fibrin and agarose scaffolds that reported the successful encapsulation of chondrocytes within these biomaterials by separate. [36-38] Furthermore, it was previously demonstrated that the combination of FAH and MNPs supports the viability and functionality of human fibroblast *ex vivo*.[16, 24]

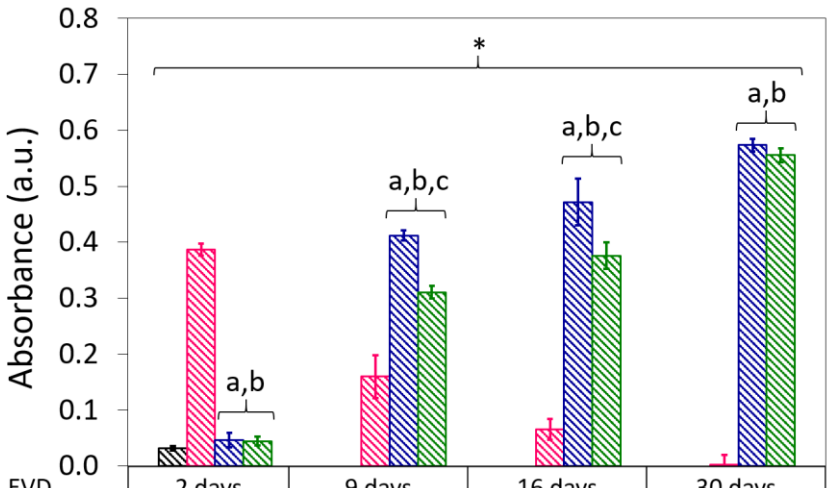

EVD	2 days	9 days	16 days	30 days
Negative CTR	0.03 ± 0.004	0.00 ± 0.000	0.00 ± 0.005	0.00 ± 0.002
Positive CTR	0.39 ± 0.011	0.16 ± 0.038	0.07 ± 0.019	0.00 ± 0.017
c-FAH	0.05 ± 0.013^{a,b}	0.41 ± 0.009^{a,b,c}	0.47 ± 0.042^{a,b,c}	0.57 ± 0.012^{a,b}
c-MFAH	0.04 ± 0.008^{a,b}	0.31 ± 0.012^{a,b,c}	0.38 ± 0.024^{a,b,c}	0.56 ± 0.012^{a,b}

Fig. 8. WST-1 quantitative and statistical results. Graphic representation of absorbance values for WST-1 assay in 2D chondrocytes cultures (positive and negative control) and experimental groups (3D chondrocyte cultures in c-FAH and c-MFAH). Values are shown as mean ± SD; $p < 0.05$ was considered statistically significant for Mann-Whitney non-parametric test. Comparisons over the time and between groups are indicated as it follows:
*= Statistically significant differences for each group over the time.
a= Statistically significant differences of experimental groups vs. negative Ctr.
b= Statistically significant differences of experimental groups vs. positive Ctr.
c= Statistically significant differences between c-FAH and c-MFAH groups

In addition, different studies indicate that the presence of MNP in scaffolds used for tissue engineering applications stimulates adhesion, proliferation, and differentiation of cells *in vitro*, and even bone formation *in vivo*. [19-22] In connection with this, recently a method for promoting osteogenesis using MNP and electromagnetic fields was patented.[39] In even more recent works it has been demonstrated the combinatory effects of a static magnetic field with the use of scaffolds containing MNP on bone regeneration.[40, 41] From a different perspective, the presence of MNP allows acting at a distance by noncontact magnetic forces. This can be used to control the structure of biomaterials. For example, Guo and Kaufman reported a technique to align collagen gels by using magnetic beads in an external magnetic field.[42] Similarly, Sharma *et al*. prepared bi-directionally oriented collagen matrices by application of a magnetic field to suspensions of magnetic nanowires in solutions of collagen during their fixation.[43] The observed bi-directional alignment was even transferred to arachnoid cells cultured in the aligned collagen matrices. More recently, Shi *et al.* reported the preparation of anisotropic collagen hydrogels by magnetic field-induced alignment of SiO_2@Fe_3O_4 rods embedded within the pre-gel solution.[18] These authors found changes in the rheological properties of hydrogels connected to rod alignment and, more interestingly, a statistically significant enhancement of cellular activity in anisotropic hydrogels with respect to

isotropic hydrogels. They connected this enhancement in cellular activity to the formation of domains defined by the aligned rods, where cell adhesion and proliferation was favored.

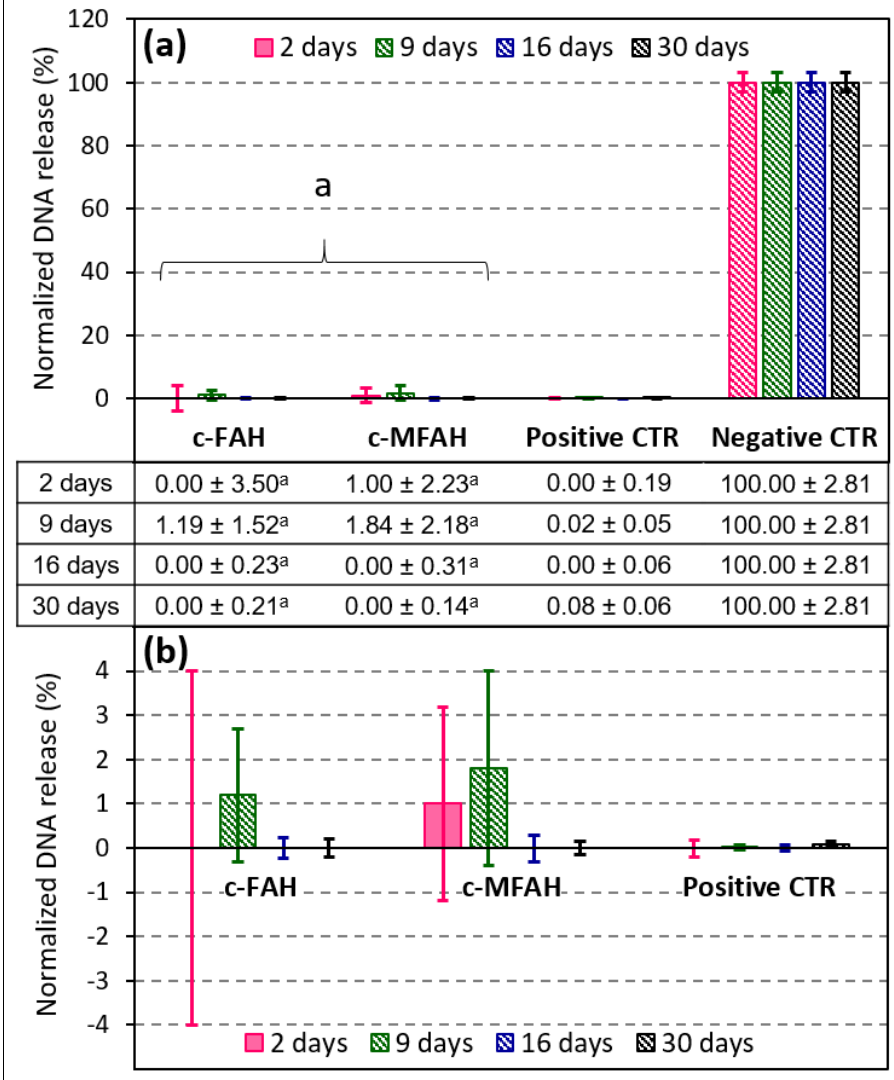

	c-FAH	c-MFAH	Positive CTR	Negative CTR
2 days	0.00 ± 3.50[a]	1.00 ± 2.23[a]	0.00 ± 0.19	100.00 ± 2.81
9 days	1.19 ± 1.52[a]	1.84 ± 2.18[a]	0.02 ± 0.05	100.00 ± 2.81
16 days	0.00 ± 0.23[a]	0.00 ± 0.31[a]	0.00 ± 0.06	100.00 ± 2.81
30 days	0.00 ± 0.21[a]	0.00 ± 0.14[a]	0.08 ± 0.06	100.00 ± 2.81

Fig. 9. Quantitative results of released DNA from HHC during 30 days of *ex vivo* cell culture. a) Graphic representation of normalized DNA values for experimental conditions, positive control and negative control groups. Data are shown as mean ± SD, normalized with respect to the negative control group (100 %).
b) Enlarged graphic representation for c-FAH, c-MFAH and positive CTR groups. In this study, $p < 0.05$ was considered statistically significant for Mann-Whitney non-parametric test. Comparisons over the time and between groups are indicated as it follows:
*= Statistically significant differences for each group over the time.
a= Statistically significant differences of experimental groups vs. negative Ctr.
b= Statistically significant differences of experimental groups vs. positive Ctr.
c= Statistically significant differences between c-FAH and c-MFAH groups

3.3. Histological cell-biomaterial interaction analyses

Morphological analyses conducted with HE staining revealed a successful encapsulation and relatively homogeneous distribution of the HHC within the FAH and MFAH during the whole length of the experiment (Fig. 10). Histology revealed that cells acquired an elongated shape with multiple cytoplasmic prolongations which clearly indicate an active cell-biomaterial interaction in FAH and MFAH (Fig. 10). In addition, the incorporation of MNPs into the FAH provided a typical granular pattern to the hydrogels, and the presence and distribution of these particles was accurately and specifically demonstrated by Perl's histochemical method (Fig. 10). During the 30 days analyzed no change in S-100 protein expression was observed, indicating that chondrocytes kept their differentiation profile in FAH and MFAH (Fig. 10). The positive interaction of HHC with FAH and MFAH was accompanied by a clear, consistent and significant increase of the number of cells in each condition over the time, especially when cells were cultured in FAH (Fig. 11). However, differences between c-FAH and c-MFAH groups along the study were not statistically significant.

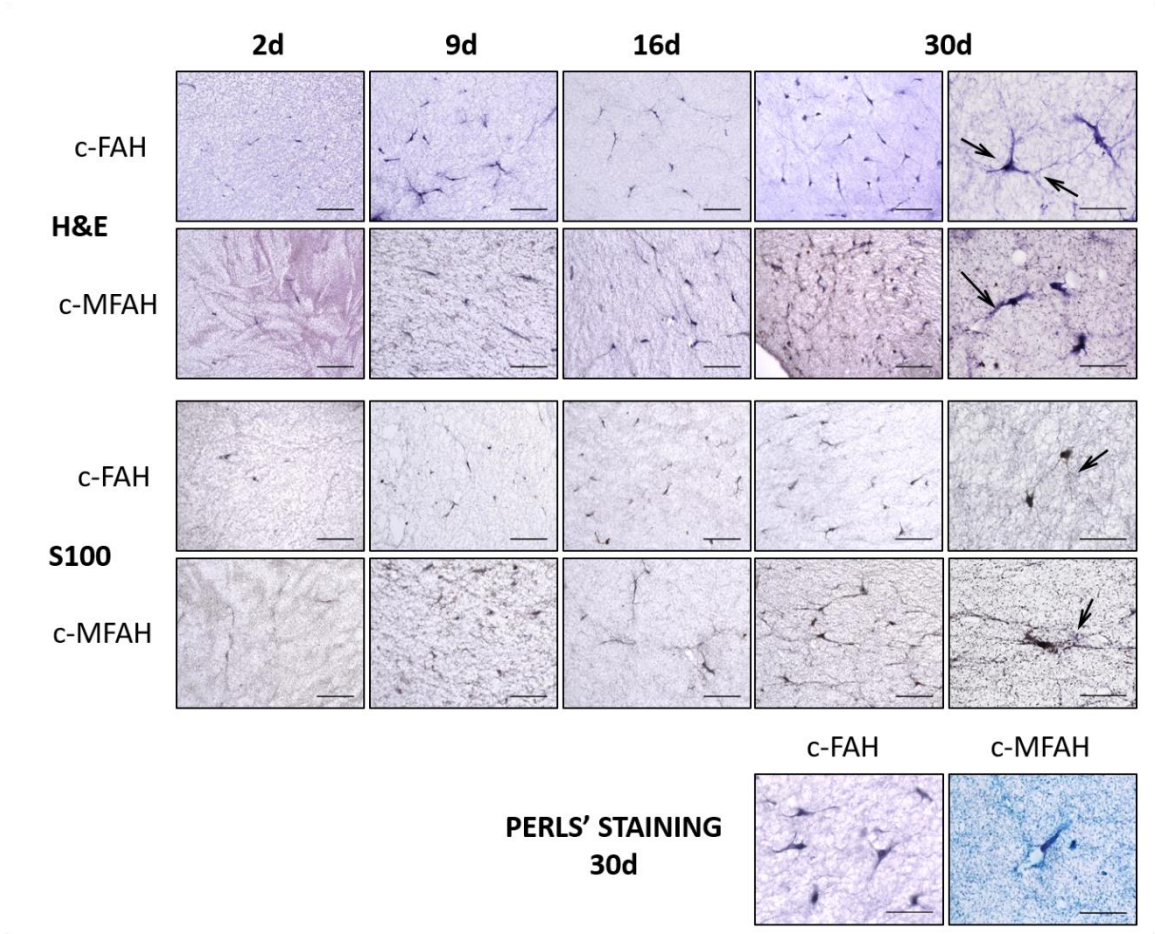

Fig. 10. Histology of c-FAH and c-MFAH during the 30 days of EVD. Hematoxylin-eosin staining, IHC for S-100 and Perl's histochemical staining for MNP visualization (blue color) are shown. Note the presence of cytoplasmic prolongations in c-FAH and c-MFAH l groups (arrows). Scale bar is 100 µm, except for the right column where scale bar is 50 µm

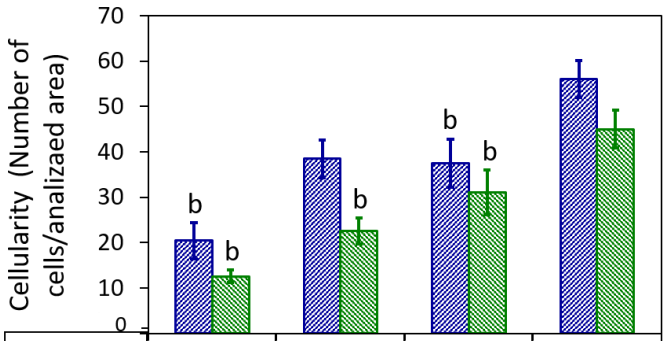

Time of IVD	2 days	9 days	16 days	30 days
c-FAH	20 ± 4[b]	38 ± 4	37 ± 5[b]	56 ± 4
c-MFAH	13 ± 1[b]	23 ± 3[b]	31 ± 5[b]	45 ± 4

Fig. 11. Cellularity (number of cells /area of 1.24 mm^2) for c-FAH and c-MFAH groups during the EVD time. Cell counting was realized from the histological sections of H&E staining. Values are shown as mean ± SD; $p < 0.05$ was considered statistically significant for Mann-Whitney non-parametric test. Comparisons over the time and between groups are indicated as it follows:
a= significant differences between c-FAH vs c-MFAH in each period of time.
b= significant differences between a determinate time vs. the consecutive time for each experimental condition.

When the synthesis of acid proteoglycans, some well-known cartilage-related ECM molecules, was evaluated, alcian blue histochemical methods did not revealed a clear positive reaction for these molecules over the time in c-FAH and c-MFAH groups (Fig. 12). However, the IHC identification of collagen type II revealed a pericellular positive reaction in both experimental conditions during the period under study, indicating the capability of these cells to produce this important and cartilage-specific ECM molecule.

Overall histological analyses are in agreement with the results obtained with WST-1 and DNA assays, demonstrating that FAH and MFAH support the viability, metabolic activity, proliferation and functionality of HHC *ex vivo*. In addition, the slight, and in most of the cases not significant differences observed between results for FAH and MFAH, could be related to the biomaterial structural and/or biomechanical properties. Indeed, cells cultured within MFAH showed a consistent increase of viability, proliferation (cellularity) and functionality (WST-1 and histology) over the time, but it was always slightly inferior to the case of FAH. In this context, rheology demonstrated that the incorporation of MNP into FAH increased the biomechanical properties (a strengthening of the structure was found –see Figs. 3 and 5) and it is well-known that this improvement is related to structural changes,[24] which were evident at the histological level. Probably, the increase of the biomaterials density due to the presence of MNP had an impact on the cell-biomaterial interactions or even nutrient or oxygen diffusion, explaining the slight differences observed between FAH and MFAH in this study. In addition, as discussed before, the active cell-biomaterial interactions (presence of abundant and long cellular processes) could explain the reduction of the volume of the hydrogels, by cell-mediated contraction, as well as the maintenance of the net strength observed in cellular FAH and MFAH constructs (see Fig. 3 and Fig. 4). This hypothesis is supported by our previous studies where the increase of FAH density by the use of nanostructuration technique resulted in a

reduction of the cell functionality and cellularity, but the cells showed a progressive adaptation to the new microenvironment with a successful recovery at the end of the study.[29] Similarly, differences in the cell function (proliferation, cellularity and synthesis of extracellular matrix) were observed in mesenchymal stem cells cultured in nanostructured FAH as compared to uncompressed FAH, demonstrating that the porosity and density of the hydrogel has a direct impact on the cell viability and functionality *ex vivo*.[27, 29] In relation to the biomaterial biodegradation, slight signs of biodegradation were observed around 30 days *ex vivo* (Figs. 10 and 12). Finally, these results suggested that the incorporation of MNP did not affect the intrinsic cytocompatibility of the fibrin-agarose matrices to develop an *in vitro* cell culture of HHC. Nevertheless, it is evident that this 3D model needs improvements in order to generate a more biomimetic and functional cartilage substitute for future preclinical applications.

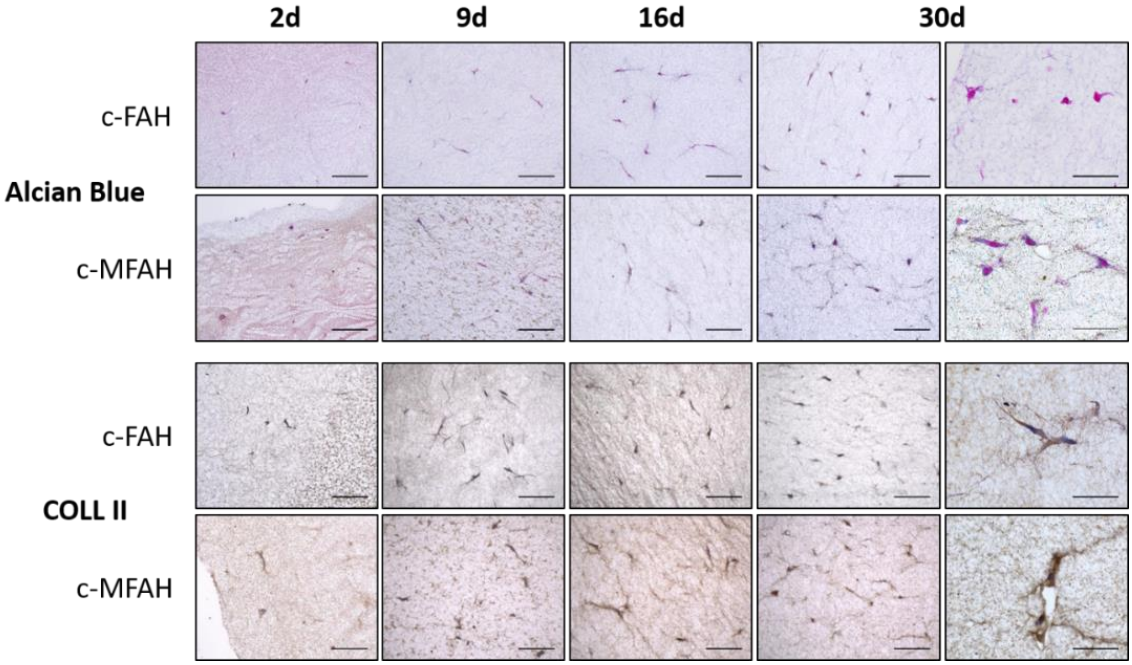

Fig. 4. Histological analysis of proteoglycans and type II collagen in c-FAH and c-MFAH groups. Note the brown pericellular positive reaction for type II collagen in c-FAH and c-MFAH groups over the time. Scale bar is 100 µm except for the right column where scale bar is 50 µm.

In view of the results obtained from the histological, histochemical and immunohistochemical analyses, we cannot conclude that an artificial articular cartilage-like tissue was obtained by embedding HHC within nonmagnetic or magnetic fibrin-agarose biomaterials (c-FAH and c-MFAH respectively). However, the expression of characteristic chondrogenic proteins by HHC such as type II collagen was observed. And, most interestingly, we found no adverse results by the inclusion of MNP within the biomaterials in terms of cell proliferation, DNA release and cellularity. Thus, we have opened a promising research line, aimed to the generation of artificial articular hyaline cartilage-like tissues with magnetic properties, which may benefit from the advantages of using embedded magnetic nanoparticles.

4. Conclusions

We have reported the generation of a first approximation of engineered hyaline cartilage-like tissues by embedding human hyaline chondrocytes within nonmagnetic and magnetic (containing 0.1 % v/v magnetic nanoparticles) fibrin-agarose hydrogels. Our analysis has shown that the inclusion of magnetic nanoparticles resulted in stronger and biomechanically stable biomaterials (higher values of the viscoelastic moduli). More interestingly, the presence of cells (cellular samples) stabilized the biomechanics of the biomaterials, by compensating the slight degradation of the polymer during the cell-culture time, by a cell-mediated contraction that resulted in a decrease of the volume of the biomaterials and stable values of the viscoelastic moduli. The obtained biomaterials were very soft viscoelastic solids (complex modulus of rigidity less than 100 Pa) which could allow, where appropriate, their implantation by injection. However, they were much weaker materials than human articular cartilage tissue (modulus of rigidity of the order of 1 MPa) and, therefore, their use as substitutes of these native tissues will still require an intense subsequent reform.

Cytotoxicity (DNA release) and cell proliferation (WST-1 test) assays were promising for magnetic biomaterials. In fact, the inclusion of magnetic nanoparticles within fibrin-agarose matrices did not negatively affect the viability and proliferation of chondrocytes. The results of both tests were similar for the positive control group (c-FAH) and the experimental magnetic group (c-MFAH). Histological analyses were performed using standard histochemical and immunohistochemical techniques. From these tests, it was obtained that the chondrocytes interacted with both tested biomaterials (c-FAH and c-MFAH), as evidenced the elongated filopodium of the HHC. The expression of S-100 protein by HHC within the biomaterials confirmed that their lineage was not lost due to the environment where the cells were encapsulated. Furthermore, the encapsulated HHC were able to express at least one of the most important proteins present in the extracellular matrix of a native cartilage (type II collagen), in both experimental and control groups.

To conclude, we generated 3D magnetic cartilage-like fibrin-agarose biomaterials with improved biomechanical properties, which are combined with magnetic character due to the presence of magnetic nanoparticles, as well as high swelling degree. Culture of human hyaline chondrocytes was viable within these biomaterials, and immunohistochemistry confirmed that these cells were able to express ECM native hyaline cartilage proteins. Nevertheless, for the culture time under study (30 days), the human hyaline chondrocytes within the biomaterials did not reach a high maturation degree and it was not possible to generate a highly biomimetic tissue engineered substitute. Our promising results should contribute to the development of the interesting line in the field of biomedicine that represents the use of magnetic biomaterials for tissue engineering applications. Other advantages linked to the presence of magnetic nanoparticles are expected for such magnetic biomaterials in the field of tissue engineering, such as potential manipulation of the microstructure by noncontact magnetic forces, or generation of mechanical stresses at the microscopic level by applied magnetic fields, which may contribute to cell proliferation and differentiation, and to a better development and application of this field of research.

Acknowledgments

This study was supported by projects FIS2013-41821-R (Plan Nacional de Investigación Científica, Desarrollo e Innovación Tecnológica, Ministerio de Economía, Industria y Competitividad, MINECO Spain, cofunded by Fondo Europeo de Desarrollo Regional, FEDER, European Union), FIS2017-85954-R (Ministerio de Economía, Industria y Competitividad, MINECO, and Agencia Estatal de Investigación, AEI, Spain, cofunded by Fondo Europeo de Desarrollo Regional, FEDER, European Union), and by the *Consejería de Salud y Familias, Junta de Andalucía, España*, Grant SAS CS PI-0257-2017.

References

1. Vinatier, C. and J. Guicheux, *Cartilage tissue engineering: From biomaterials and stem cells to osteoarthritis treatments.* Annals of physical and rehabilitation medicine, 2016. **59**(3): p. 139-44.
2. Mackie, E.J., L. Tatarczuch, and M. Mirams, *The skeleton: a multi-functional complex organ. The growth plate chondrocyte and endochondral ossification.* Journal of Endocrinology, 2011. **211**(2): p. 109-121.
3. Landínez Parra, N.S., D.A. Garzón-Alvarado, and J.C. Vanegas Acosta, *Phenomenology work setting for articular cartilage damage. Marco de trabajo fenomenológico para el daño del cartílago articular.* Revista Cubana de Ortopedia y Traumatología, 2009. **23**(2): p. 0-0.
4. Mills and Stacey, *Histology for Pathologists*. 5th Ed. ed. 2019: Lippincott Williams & Wilkins (LWW).
5. Becerra, J., et al., *Articular Cartilage: Structure and Regeneration.* Tissue Engineering Part B-Reviews, 2010. **16**(6): p. 617-627.
6. Chapman, V., et al., *Therapeutic Benefit for Late, but Not Early, Passage Mesenchymal Stem Cells on Pain Behaviour in an Animal Model of Osteoarthritis.* Stem Cells International, 2017.
7. Lories, R.J. and F.P. Luyten, *The bone-cartilage unit in osteoarthritis.* Nature Reviews Rheumatology, 2011. **7**(1): p. 43-49.
8. Hochberg, Z., *Clinical physiology and pathology of the growth plate.* Best Practice & Research Clinical Endocrinology & Metabolism, 2002. **16**(3): p. 399-419.
9. Stoltz, J.F., et al., *Mechanobiology and cartilage engineering: The underlying pathophysiological phenomena.* Biorheology, 2006. **43**(3-4): p. 171-180.
10. Johnstone, B., et al., *TISSUE ENGINEERING FOR ARTICULAR CARTILAGE REPAIR - THE STATE OF THE ART.* European Cells & Materials, 2013. **25**: p. 248-267.
11. Widuchowski, W., J. Widuchowski, and T. Trzaska, *Articular cartilage defects: Study of 25,124 knee arthroscopies.* Knee, 2007. **14**(3): p. 177-182.
12. Khan, F. and S.R. Ahmad, *Polysaccharides and Their Derivatives for Versatile Tissue Engineering Application.* Macromolecular Bioscience, 2013. **13**(4): p. 395-421.
13. Makris, E.A., et al., *Repair and tissue engineering techniques for articular cartilage.* Nature Reviews Rheumatology, 2015. **11**(1): p. 21-34.
14. Chato-Astrain, J., et al., *In vivo Evaluation of Nanostructured Fibrin-Agarose Hydrogels With Mesenchymal Stem Cells for Peripheral Nerve Repair.* Frontiers in Cellular Neuroscience, 2018. **12**.
15. Garcia-Martinez, L., et al., *Encapsulation of human elastic cartilage-derived chondrocytes in nanostructured fibrin-agarose hydrogels.* Histochem Cell Biol, 2017. **147**(1): p. 83-95.

16. Rodriguez-Arco, L., et al., *Biocompatible magnetic core-shell nanocomposites for engineered magnetic tissues.* Nanoscale, 2016. **8**(15): p. 8138-8150.
17. Shimizu, K., A. Ito, and H. Honda, *Enhanced cell-seeding into 3D porous scaffolds by use of magnetite nanoparticles.* Journal of Biomedical Materials Research Part B-Applied Biomaterials, 2006. **77B**(2): p. 265-272.
18. Shi, Y., Y. Li, and T. Coradin, *Magnetically-oriented type I collagen-SiO2@Fe3O4 rods composite hydrogels tuning skin cell growth.* Colloids and Surfaces B: Biointerfaces, 2020. **185**: p. 110597.
19. Perez, R.A., K.D. Patel, and H.W. Kim, *Novel magnetic nanocomposite injectables: calcium phosphate cements impregnated with ultrafine magnetic nanoparticles for bone regeneration.* Rsc Advances, 2015. **5**(18): p. 13411-13419.
20. Singh, R.K., et al., *Potential of Magnetic Nanofiber Scaffolds with Mechanical and Biological Properties Applicable for Bone Regeneration.* Plos One, 2014. **9**(4).
21. Bañobre-Lopez, M., et al., *Poly(caprolactone) based magnetic scaffolds for bone tissue engineering.* Journal of Applied Physics, 2011. **109**(7): p. 07B313.
22. De Santis, R., et al., *A route toward the development of 3D magnetic scaffolds with tailored mechanical and morphological properties for hard tissue regeneration: Preliminary study A basic approach toward the design of 3D rapid prototyped magnetic scaffolds for hard- tissue regeneration is presented and validated in this paper.* Virtual and Physical Prototyping, 2011. **6**(4): p. 189-195.
23. Garzon, I., et al., *A combined approach for the assessment of cell viability and cell functionality of human fibrochondrocytes for use in tissue engineering.* PLoS One, 2012. **7**(12): p. e51961.
24. Bonhome-Espinosa, A.B., et al., *Effect of particle concentration on the microstructural and macromechanical properties of biocompatible magnetic hydrogels.* Soft Matter, 2017. **13**(16): p. 2928-2941.
25. Berneel, E., et al., *Redifferentiation of High-Throughput Generated Fibrochondrocyte Micro-Aggregates: Impact of Low Oxygen Tension.* Cells Tissues Organs, 2016. **202**(5-6): p. 369-381.
26. Campos, F., et al., *Ex vivo characterization of a novel tissue-like cross-linked fibrin-agarose hydrogel for tissue engineering applications.* Biomed Mater, 2016. **11**(5): p. 055004.
27. Campos, F., et al., *Generation of genipin cross-linked fibrin-agarose hydrogel tissue-like models for tissue engineering applications.* Biomedical Materials, 2018. **13**(2).
28. Carriel, V., et al., *Tissue Fixation and Processing for the Histological Identification of Lipids.* Methods Mol Biol, 2017. **1560**: p. 197-206.
29. Carriel, V., et al., *In vitro characterization of a nanostructured fibrin agarose bio-artificial nerve substitute.* Journal of Tissue Engineering and Regenerative Medicine, 2017. **11**(5): p. 1412-1426.
30. Edelstein, A.D., et al., *Advanced methods of microscope control using μManager software. .* Journal of Biological Methods, 2014. **1**(2): p. e10.
31. Rubistein, M. and R.H. Colby, *Polymer Physics*. 2003: Oxford University, New York, NY.
32. Macosko, C.W., *Rheology: Principles, Measurements and Applications*. 1994: Wiley-VCH, Weinheim.
33. Barnes, H.A., J.F. Hutton, and K. Walters, *An Introduction to Rheology*. 1989: Elsevier.
34. Stammen, J.A., et al., *Mechanical properties of a novel PVA hydrogel in shear and unconfined compression.* Biomaterials, 2001. **22**(8): p. 799-806.
35. Magnussen, R.A., F. Guilak, and T.P. Vail, *Cartilage degeneration in post-collapse cases of osteonecrosis of the human femoral head: Altered mechanical properties in tension, compression, and shear.* Journal of Orthopaedic Research, 2005. **23**(3): p. 576-583.
36. Scotti, C., et al., *Effect of in vitro culture on a chondrocyte-fibrin glue hydrogel for cartilage repair.* Knee Surgery Sports Traumatology Arthroscopy, 2010. **18**(10): p. 1400-1406.

37. Eyrich, D., et al., *Long-term stable fibrin gels for cartilage engineering.* Biomaterials, 2007. **28**(1): p. 55-65.
38. Mesa, J.M., et al., *Tissue engineering cartilage with aged articular chondrocytes in vivo.* Plastic and Reconstructive Surgery, 2006. **118**(1): p. 41-49.
39. Hyun, J., et al., *Method for promoting osteogenesis using magnetic nanoparticles and electromagnetic field*. 2015: World patent.
40. Yun, H.-M., et al., *Magnetic nanocomposite scaffolds combined with static magnetic field in the stimulation of osteoblastic differentiation and bone formation.* Biomaterials, 2016. **85**: p. 88-98.
41. Hao, S., et al., *Macrophage phenotypic mechanomodulation of enhancing bone regeneration by superparamagnetic scaffold upon magnetization.* Biomaterials, 2017. **140**: p. 16-25.
42. Guo, C. and L.J. Kaufman, *Flow and magnetic field induced collagen alignment.* Biomaterials, 2007. **28**(6): p. 1105-1114.
43. Sharma, A., et al., *Alignment of collagen matrices using magnetic nanowires and magnetic barcode readout using first order reversal curves (FORC) (invited).* Journal of Magnetism and Magnetic Materials, 2018. **459**: p. 176-181.